

An Improved Algorithm for Deducing Complex Permittivity of Thin Dielectric Samples with the Transmission/Reflection Method

Minghui Ding¹, Yanqing Liu², Xinru Lu¹, Yifeng Li³, and Weizhong Tang^{1, *}

Abstract—Transmission/reflection method is widely used in microwave engineering for determining dielectric properties of materials, and significant uncertainty will arise in the results if the thickness of the samples is small. In this paper, we propose an improved algorithm for deducing complex permittivity of thin dielectric samples with the transmission/reflection method. With the proposed algorithm, the real and imaginary parts of the complex permittivity will be treated separately, and two independent weighting factors, β_{re} and β_{im} , will be used to minimize the uncertainty in both parts of the complex permittivity. Numerical calculations as well as experimental measurements on undoped and boron-doped diamond films were conducted within the frequency range of 18.5–26.5 GHz to demonstrate the effectiveness of the algorithm. It is verified that among the various iterative algorithms which could be used to derive complex permittivity, the proposed algorithm is the most advantageous in reducing uncertainties when thin dielectric samples are dealt with.

1. INTRODUCTION

Determination of a material's dielectric property is a prerequisite for application of the material in the field of microwave engineering. For this reason, many measuring techniques have been developed which could generally be divided into two groups, i.e., resonant and non-resonant methods [1]. Among the various techniques, the transmission/reflection (T/R) method is widely used because of its simplicity in equipment and capability in wideband measurements.

In the T/R measurement, a sample is inserted into either a waveguide, a coaxial line or a striplining, and complex permittivity of the sample will be deduced from scattering parameters (S -parameters) measured at the two ends of the measurement fixture. This method was first proposed by Nicolson and Ross [2], and Weir [3], so was given the name NRW algorithm. During the last decades, progressive improvements have been made on the T/R method [4–12]. Baker-Jarvis et al. [9] proposed an iterative approach to eliminate the ill-behavior of the original NRW algorithm. They showed that by incorporating a weighting factor β into the algorithm, the uncertainty of the complex permittivity derived from the algorithm could be effectively reduced. Later on, Kato et al. [10] proposed an alternative approach in selecting the weighting factor, in order to further minimize the uncertainty in determining the complex permittivity. However, by referring to the results shown in [10], it can be seen that the uncertainty of the imaginary part of the complex permittivity determined in such a way may not necessarily be decreased, though uncertainty in the real part of the result may be reduced.

Generally speaking, even with an iterative algorithm, significant uncertainty will arise in deriving the complex permittivity, if the thickness of the sample is small. In this paper, we propose a further improvement on the iterative algorithms developed by Baker-Jarvis et al. [9] and Kato et al. [10]. In

Received 18 June 2019, Accepted 13 August 2019, Scheduled 20 August 2019

* Corresponding author: Weizhong Tang (wztang@mater.ustb.edu.cn).

¹ Institute for Advanced Materials and Technology, University of Science and Technology Beijing, Beijing 100083, China. ² Institute of Interdisciplinary Information Sciences, Tsinghua University, Beijing 100084, China. ³ Institute of Laser Technology, Academy of Sciences of Hebei Province, Shijiazhuang 050081, China.

our approach, the real and imaginary parts of the complex permittivity will be treated separately, and two weighting factors, β_{re} and β_{im} , will be employed in the iterative calculation, so as to decrease the uncertainty in both the real and imaginary parts of the complex permittivity. Uncertainty analysis will be conducted by numerical calculations, showing that with the proposed algorithm both the real and imaginary parts of the complex permittivity of thin samples may be more accurately determined than those derived using alternative algorithms. Experimental measurements are carried out on thin undoped and boron-doped diamond films to prove the effectiveness of the improved algorithm in measuring complex permittivity of thin dielectric samples.

2. THEORETICAL BACKGROUND

Figure 1 shows a schematic of the T/R method in measuring dielectric properties of a sample within a rectangular waveguide. The situations with a coaxial line [9] or a stripline [13] as measurement fixtures may be similarly treated. In the figure, L is the thickness of the sample with a relative complex permittivity ϵ_r and relative complex permeability μ_r ; L_a is the length of the waveguide fixture; L_1 and L_2 are the distances between the sample surfaces and the relevant reference planes (port 1 and 2), respectively. S -parameters (S_{ij} , $i, j = 1, 2$) are measured at ports 1 and 2 by using a vector network analyzer connected to the waveguide fixture.

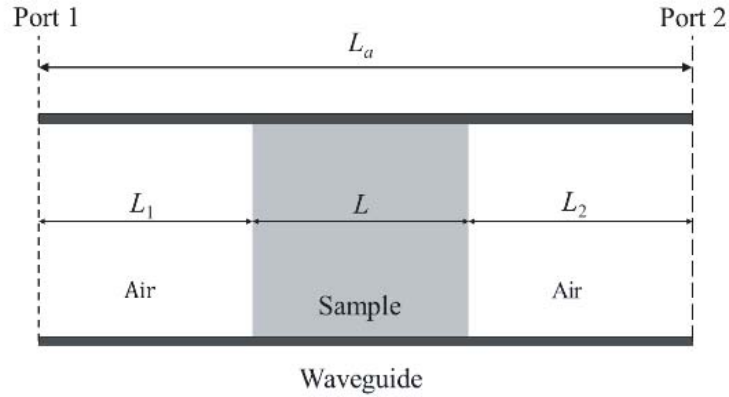


Figure 1. Schematic of the T/R method with a rectangular waveguide as the measurement fixture.

One of the most widely used equations derived by Baker-Jarvis et al. [9] for determining the complex permittivity ϵ_r of the sample is of the form:

$$S_{12}S_{21} - S_{11}S_{22} = \frac{z^2 - \Gamma^2}{1 - \Gamma^2 z^2} \exp[2\gamma_0(L_a - L)] \quad (1)$$

where $\Gamma = (\gamma_0 - \gamma)/(\gamma_0 + \gamma)$ and $z = \exp(-\gamma L)$ are the reflection coefficient and propagation factor, and γ_0 and γ are the propagation constants of microwave in air and in the sample, respectively. The latter two parameters are related to the complex permittivity ϵ_r and complex permeability μ_r of the sample by relations shown below:

$$\gamma_0 = j\sqrt{(\omega/c)^2 - (2\pi/\lambda_c)^2}, \quad \gamma = j\sqrt{(\omega/c)^2 \epsilon_r \mu_r - (2\pi/\lambda_c)^2} \quad (2)$$

where c is the speed of light in vacuum and ω the microwave angular frequency, and λ_c the cutoff wavelength of the waveguide. In the following, we deal only with the situation in which the sample is made of a nonmagnetic material, thus we have $\mu_r = 1$

In order to improve accuracy of the calculation, another equation containing a weighting factor β may be used [9]:

$$\frac{1}{2} \{ \exp[\gamma_0(L_a - L)](S_{12} + S_{21}) + \beta \{ S_{11} + \exp[2\gamma_0(L_a - L)] S_{22} \} \} = \frac{z(1 - \Gamma^2) + \beta \Gamma(1 - z^2)}{1 - \Gamma^2 z^2} \quad (3)$$

Application of this equation requires that the condition $L_1 = 0$ is satisfied.

Both Eqs. (1) and (3) are complex functions from which complex permittivity of the sample is to be deduced. We see from these equations that S -parameters, L_a , L , and their uncertainties would affect accuracy of the derived complex permittivity through their uncertainty transfer coefficients (UTCs, denoted as partial derivatives in [9]). Air gaps between the sample and measurement fixture walls may also contribute to the uncertainties of the result. But the latter problem has been thoroughly treated in the literature [14], so in this paper this effect will no longer be discussed.

After rewriting Eq. (3) in the form of $F(\varepsilon_r, L, L_a, S, \beta) = 0$, UTCs between all variables may be derived. For example, the UTC of the real part of the complex permittivity, ε'_r , to one of the S -parameters, S_{21} , may be written as:

$$\frac{\partial \varepsilon'_r}{\partial |S_{21}|} = \text{Re} \left\{ \frac{\frac{1}{2} \exp[\gamma_0 (L_a - L)] e^{j\theta_{21}}}{\partial F / \partial \varepsilon_r} \right\}, \quad \frac{\partial \varepsilon'_r}{\partial \theta_{21}} = j |S_{21}| \frac{\partial \varepsilon'_r}{\partial |S_{21}|} \quad (4)$$

where $|S_{21}|$ and θ_{21} are the amplitude and argument of scattering parameter S_{21} . All other UTCs of every parameter could be derived similarly. After all UTCs are obtained, uncertainties in the real and imaginary parts of the complex permittivity may be expressed:

$$\Delta \varepsilon'_r = \sqrt{\sum_{i,j} \left\{ \left(\frac{\partial \varepsilon'_r}{\partial |S_{ij}|} \Delta |S_{ij}| \right)^2 + \left(\frac{\partial \varepsilon'_r}{\partial \theta_{ij}} \Delta \theta_{ij} \right)^2 \right\} + \left(\frac{\partial \varepsilon'_r}{\partial L} \Delta L \right)^2 + \left(\frac{\partial \varepsilon'_r}{\partial L_a} \Delta L_a \right)^2} \quad (5)$$

$$\Delta \varepsilon''_r = \sqrt{\sum_{i,j} \left\{ \left(\frac{\partial \varepsilon''_r}{\partial |S_{ij}|} \Delta |S_{ij}| \right)^2 + \left(\frac{\partial \varepsilon''_r}{\partial \theta_{ij}} \Delta \theta_{ij} \right)^2 \right\} + \left(\frac{\partial \varepsilon''_r}{\partial L} \Delta L \right)^2 + \left(\frac{\partial \varepsilon''_r}{\partial L_a} \Delta L_a \right)^2} \quad (6)$$

where $i = \{1, 2\}$, $j = \{1, 2\}$, and ε''_r is the imaginary part of the complex permittivity.

It is clear from Eq. (4) that any change in the weighting factor β would change relevant UTCs which would affect overall uncertainties of the ultimate results. Therefore, the weighting factor β should be optimally determined.

In [9], it is suggested that β is chosen as the ratio between the uncertainties of two S -parameters, $\Delta |S_{21}| / \Delta |S_{11}|$. Choice of β in this way would decrease the overall uncertainty of the complex permittivity by weighting heavily on the S -parameter with less uncertainty. However, Kato et al. [10] pointed out that a so-determined β may not be optimal. They suggested that β is chosen to minimize $(\Delta \varepsilon'_r)^2 + (\Delta \varepsilon''_r)^2$ the sum of the squares of uncertainties in both the real and imaginary parts of the complex permittivity. However, as we will show in the next section, choice of β in this way may not necessarily mean that the uncertainties in both the real and imaginary parts of the complex permittivity are decreased.

To circumvent the problem, in this paper we propose a further improvement on the choice of β . In our approach, two distinct weighting factors, β_{re} and β_{im} , will be used separately to optimize the real and imaginary parts of the complex permittivity. In other words, β_{re} will be chosen to minimize $\Delta \varepsilon'_r$, so does β_{im} to minimize $\Delta \varepsilon''_r$. Similar to the situation in [10], the uncertainties $\Delta \varepsilon'_r$ and $\Delta \varepsilon''_r$ could be derived as follows:

$$(\Delta \varepsilon'_r)^2 = \frac{c_1 + c_2 \beta_{re} + c_3 \beta_{re}^2}{c_4 + c_5 \beta_{re} + c_6 \beta_{re}^2} \quad (7)$$

$$(\Delta \varepsilon''_r)^2 = \frac{c_7 + c_8 \beta_{im} + c_9 \beta_{im}^2}{c_{10} + c_{11} \beta_{im} + c_{12} \beta_{im}^2} \quad (8)$$

where c_1, c_{12} are coefficients dependent on L, L_a, ε_r, S -parameters, and their uncertainties, but independent of the weighting factors. Thus, two distinct weighting factors, β_{re} and β_{im} , may be selected to minimize $\Delta \varepsilon'_r$ and $\Delta \varepsilon''_r$ separately, and then these two weighting factors are used to derive two complex permittivities, ε_{r1} and ε_{r2} . Finally, a new complex permittivity, $\varepsilon_r = \varepsilon'_{r1} - j\varepsilon''_{r2}$, will be formed by combining the real and imaginary parts of the two permittivities. In such a way, uncertainties in both parts of the complex permittivity may be minimized.

3. NUMERICAL CALCULATIONS

Numerical calculation is made for a thin dielectric sample with a complex permittivity of $\epsilon_r = 2(1-j0.1)$. Dimensions of the measurement are assumed as follows: $L = 0.6$ mm, $L_a = 4.5$ mm, and $L_1 = 0$. The frequency range is assumed in the K -band (18–26.5 GHz). Within this frequency range, the thickness of the sample is comparatively small (less than 10% of the microwave wavelength in the sample), so significant uncertainty will arise.

In the calculation, uncertainties in S -parameters are derived for an Agilent N5244a vector network analyzer [15], and uncertainties in dimensions are assumed as $\Delta L = 0.01$ mm and $\Delta L_a = 0.02$ mm, respectively. Fig. 2 shows uncertainties calculated for the real and imaginary parts of the complex permittivity together with weighting factors obtained by the different algorithms as a function of frequency. In the following, these three algorithms based on using Eq. (3) will be designated as the Baker-Jarvis method (β_{BJ}), Kato method (β_{Kato}), and proposed method, respectively. For the sake of comparison, the algorithm by using Eq. (1) has also been included.

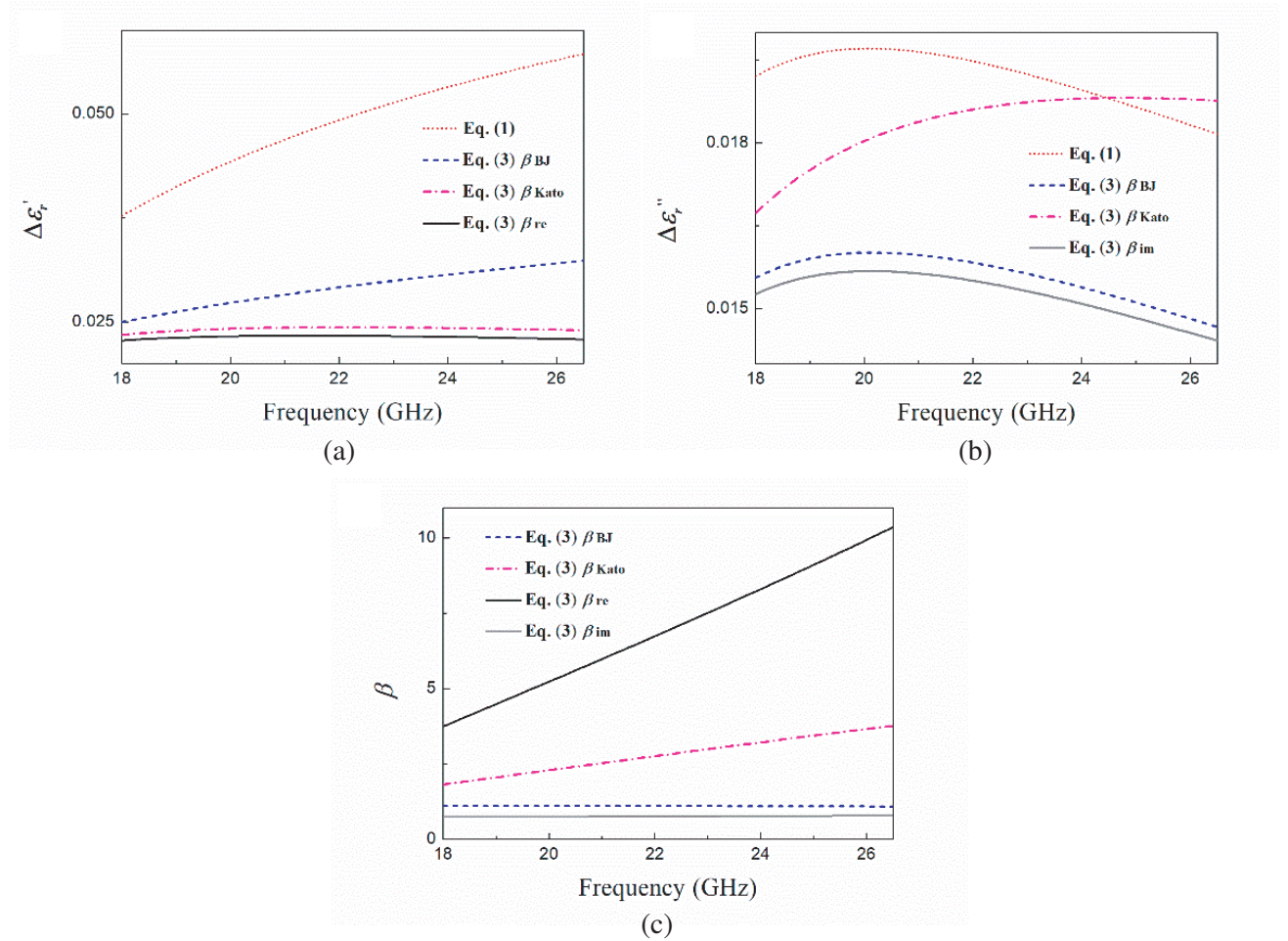


Figure 2. Uncertainties in (a) the real and (b) imaginary part of the complex permittivity and (c) the weighting factors vs frequency.

Figure 2(a) shows the uncertainty calculated for the real part of the complex permittivity. It could be noticed immediately that over the entire K -band the uncertainty is the largest for the result obtained from using Eq. (1) and the lowest obtained with the proposed method. On the other hand, while the accuracy of the calculation is improved by using either the Kato or the Baker-Jarvis method as compared with that obtained with Eq. (1), it is with the Kato method that the result is more accurate.

The latter result is consistent with that obtained in the literature [10].

Figure 2(b) shows the uncertainty calculated for the imaginary part of the complex permittivity. It is striking to see that the uncertainty obtained with the Kato method is higher than that with the Baker-Jarvis method, consistent again with the result of the literature [10]. And among all the algorithms used in the calculation, the proposed method results in the lowest uncertainty. This is because the method separates the optimization process for the real and imaginary parts of the calculation, thus avoiding their interference and improving accuracy of the results. It can also be seen from Fig. 2(b) that the uncertainty in the imaginary part of the complex permittivity obtained with the Kato method is either very close to or even higher than that derived by using Eq. (1) at high frequencies (> 25 GHz). This proves that if the weighting factor in Eq. (3) is not properly selected, accuracy of the results will not necessarily be improved, as compared with that obtainable with the conventional algorithm (Eq. (1)).

Figure 2(c) compares weighting factors obtained with the three different algorithms. It could be seen that, firstly, the two weighting factors obtained with the proposed method are quite different, while those obtained with the Kato and Baker-Jarvis methods are in between these two weighting factors. Secondly, the weighting factor obtained with the Baker-Jarvis method is very close to β_{im} , and this is also reflected in the fact that the uncertainties in the imaginary part of the permittivity obtained with both the Baker-Jarvis and the proposed method are close to each other. Since with the proposed method, two weighting factors have been used to calculate the real and imaginary parts of the complex permittivity, respectively, the uncertainties in both parts of the results may be simultaneously the lowest.

4. A SIMPLE EXPLANATION OF THE PROPOSED ALGORITHM

Above, we have proposed that in using the iterative approach in solving Eq. (3), two weighting factors, β_{re} and β_{im} , may be used separately to deduce the real and imaginary parts of the complex permittivity. In the following, rationality of the proposed algorithm will be briefly discussed.

We firstly rewrite Eq. (3) in its general form as

$$F(\epsilon'_r, \epsilon''_r, L, L_a, S, \beta) = 0 \tag{9}$$

where the weighting factor β has been incorporated to improve the accuracy of the complex permittivity caused by measurement uncertainties in dimensions and S -parameters. Thus, the uncertainties of the real and imaginary parts of complex permittivity will all be β dependent (Eqs. (7) and (8)). Fig. 3 shows schematically the interrelationship between the uncertainties in the real and imaginary parts of

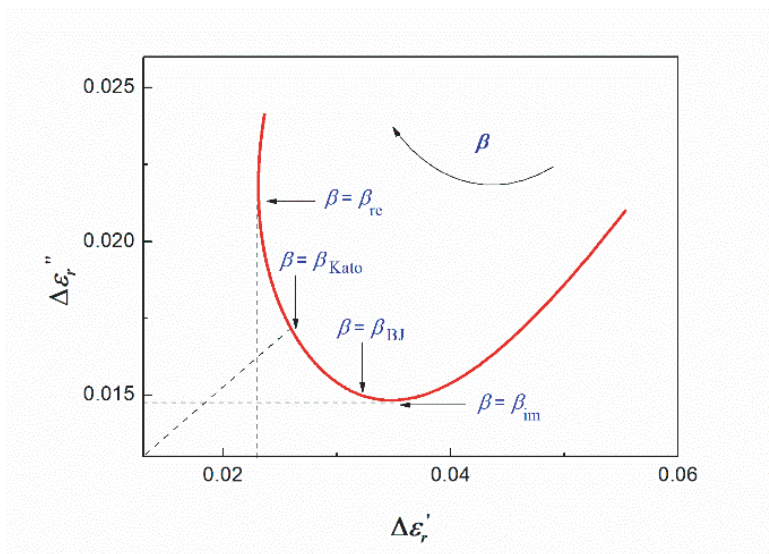


Figure 3. Curve of the uncertainties of the complex permittivity vs. β , with the data taken from Fig. 2 for a fixed frequency of 25 GHz.

the permittivity and weighting factor β . The result has been calculated using the data taken from Fig. 2 for a frequency of 25 GHz.

Just as in Kato's algorithm [10] in deducing the permittivity, we may impose the following restriction

$$(\Delta\varepsilon'_r)^2 + (\Delta\varepsilon''_r)^2 = \min \quad (10)$$

In such a procedure, a specific weighting factor β_{kato} will be obtained. It can be seen from Fig. 3 that Eq. (3) corresponds to the nearest distance of the curve to the origin. It could be noted from Fig. 3 that at this time both $\Delta\varepsilon'_r$ and $\Delta\varepsilon''_r$ are not the minimum. Instead, another form of restriction may be imposed, such as

$$(\Delta\varepsilon'_r)^2 = \min \quad (11)$$

This time, the permittivity will be deduced aiming to minimize the uncertainty in the real part of the permittivity (with a new weighting factor β_{re}), as indicated also in Fig. 3. It should be emphasized that the thus obtained real part of the permittivity (together with its uncertainty) will be valid irrespective of whether its imaginary counterpart will be explicitly used or not. This is because the thus deduced real part of the permittivity (and its uncertainty) has been calculated using the basic equation (Eq. (9)).

Likewise, a similar restriction may be imposed in solving Eq. (9):

$$(\Delta\varepsilon''_r)^2 = \min \quad (12)$$

aiming to minimize the uncertainty in the imaginary part of the permittivity. The result with the weighting factor β_{im} obtained is also indicated in Fig. 3. The thus obtained imaginary part of the permittivity (with its uncertainty) will remain valid irrespective of whether its real counterpart will be explicitly stated or not, since it has been calculated from the basic equation (Eq. (9)).

It could be imagined that in using the Baker-Jarvis' algorithm [9] the result derived for the complex permittivity (together with a weighting factor β_{BJ}) will also be located somewhere along the curve shown in Fig. 3. However, according to the former discussions the algorithm has been unable to minimize uncertainties in both parts of the permittivity either individually or collectively.

Thus, it can be seen that among all the algorithms, the proposed algorithm is the most effective in minimizing uncertainties in deducing complex permittivity of thin samples.

5. DETERMINATIONS OF PERMITTIVITY OF DIAMOND FILMS

Above we have shown that whereas various iterative algorithms may be used to deduce complex permittivity for thin dielectric samples, an improved algorithm may be employed to improve the accuracy of the results. To validate this conclusion, measurements are made on an undoped and a boron-doped diamond film. These two samples have been selected since firstly the thickness of the two samples is small, and secondly while the undoped diamond film may be used as a standard sample, the boron-doped diamond film may be used as a representative high dielectric loss sample.

In the measurements, an Agilent N5244a vector network analyzer is used. A Thru-Reflect-Line calibration procedure [10] is carried out before the measurements. Samples are inserted into a K -band waveguide fixture with a length of $L_a = 4.5$ mm. From measured S -parameters, complex permittivity of the samples is derived using the various algorithms mentioned above. Dimension uncertainties in both the fixture and the samples are $\Delta L_a = 0.02$ mm, $\Delta L = 0.01$ mm, respectively.

Figure 4 shows the results derived with the various algorithms for the undoped diamond film. The thickness of the sample is only 0.37 mm. It is shown by using resonant cavity methods that an undoped diamond film will have a relative permittivity between 5.5 and 5.7, and its dielectric loss tangent is less than 10^{-4} [16–19]. In Figs. 4(a), (c), we see that the uncertainty in the real part of the permittivity derived by using Eq. (1) remains the largest, while that obtained with the proposed method is the lowest. Also, from Fig. 4(a) we see that the real part of the permittivity derived by the proposed method is in the range of 5.51 ± 0.15 which not only has the smallest uncertainty, but also is frequency independent. This is consistent with the results of the literature [18]. In contrary, all results derived with the other methods somewhat show frequency dependency.

Also, from Fig. 4(d) we see that the uncertainty deduced by our methodology for the imaginary part of the permittivity is the lowest among all the methodologies compared. This proves that the

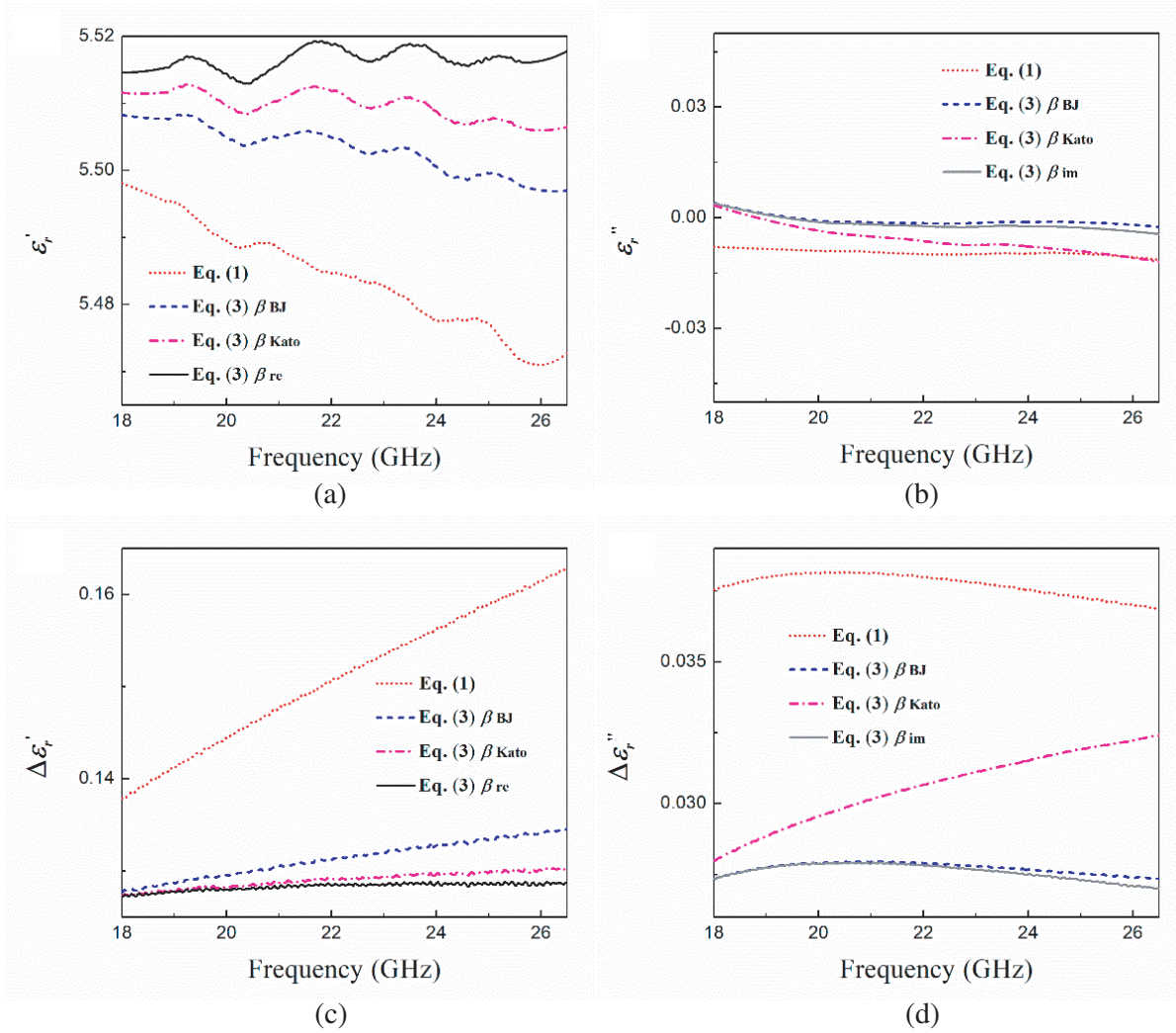


Figure 4. (a) The real and (b) imaginary part of the complex permittivity and (c), (d) their uncertainties measured for the undoped diamond film.

proposed algorithm is better than all the others. On the other hand, from Fig. 4(c) we notice that the values of the imaginary part of the complex permittivity derived by all the four algorithms are physically meaningless (far from the accurate value $\epsilon_r'' \approx 0.0003$ measured by using a split-cylinder resonator [19]). This discrepancy is because the non-resonant T/R method is limited in its accuracy in measuring the imaginary part of the complex permittivity when being used to characterize low-loss materials [20].

Figure 5 shows the results of the complex permittivity and corresponding uncertainties for the boron doped diamond film. The thickness of this sample is 0.46 mm, and its boron concentration has been determined by FT-IR as $6.0 \times 10^{18} \text{ cm}^{-3}$ [21]. From Figs. 5(a), (b), we see that for this high-loss diamond film sample, both the real and imaginary parts of the complex permittivity are frequency dependent, irrespective of the algorithms used. This is explained by considering two contributions, i.e., the hopping polarization of bound charges and valence band conduction of free charge carriers exist in the boron doped diamond film [21]. From Fig. 5, we see once again that the results derived by using Eq. (1) have the highest uncertainties in both the real and imaginary parts of the complex permittivity. On the other hand, though both the Baker-Jarvis and Kato algorithms may be used to improve accuracy of the results, the most accurate results are the ones obtained with the proposed algorithm.

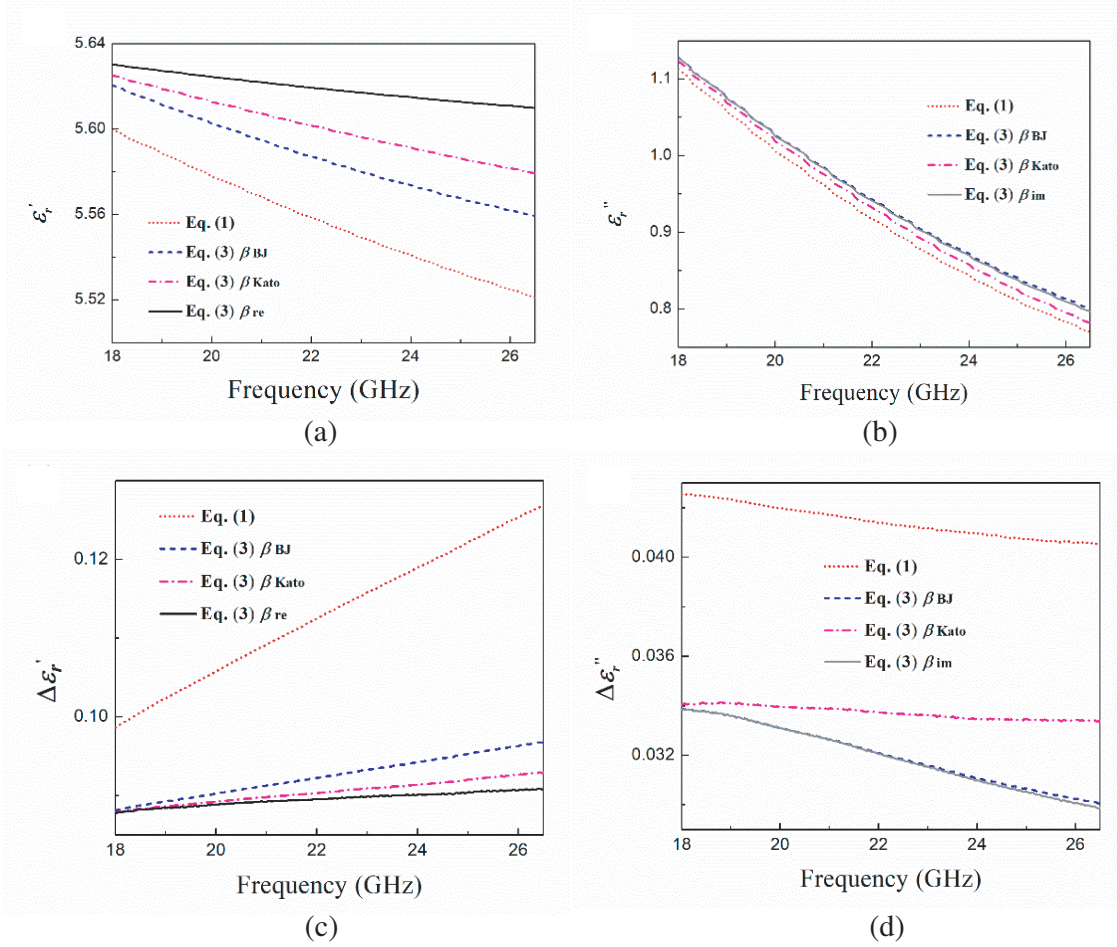


Figure 5. (a) The real and (b) imaginary part of the complex permittivity and (c), (d) their uncertainties measured for the boron doped diamond film.

6. CONCLUSIONS

In this paper, an improved iterative algorithm for deducing complex permittivity of thin dielectric samples is proposed. The improvement has been made on the algorithms previously developed by Baker-Jarvis et al. and Kato et al. It is shown that by using two distinct weighting factors separately in determining the real and imaginary part of the complex permittivity, more accurate results may be obtained. Numerical calculations are carried out, and experimental measurements are made on two thin diamond film samples, proving that the proposed algorithm is effective in reducing measurement uncertainty in measuring dielectric properties of thin samples with the T/R method.

REFERENCES

1. Chen, L. F., C. K. Ong, C. P. Neo, V. V. Varadan, and V. K. Varadan, *Microwave Electronics: Measurement and Materials Characterization*, John Wiley & Sons, Ltd, England, 2004.
2. Nicolson, A. M. and G. F. Ross, "Measurement of the intrinsic properties of materials by time-domain techniques," *IEEE Transactions on Instrumentation and Measurement*, Vol. 19, 377–382, 1970.
3. Weir, W. B., "Automatic measurement of complex dielectric constant and permeability at microwave frequencies," *Proceedings of the IEEE*, Vol. 62, 33–36, 1974.

4. Kim, S. and J. R. Guerrieri, "Low-loss complex permittivity and permeability determination in transmission/reflection measurements with time-domain smoothing," *Progress In Electromagnetics Research M*, Vol. 44, 69–79, 2015.
5. Hasar, U. C., J. J. Barroso, C. Sabah, and Y. Kaya, "Resolving phase ambiguity in the inverse problem of reflection-only measurement methods," *Progress In Electromagnetics Research*, Vol. 129, 405–420, 2012.
6. Kim, S. and J. Baker-Jarvis, "An approximate approach to determining the permittivity and permeability near $\lambda/2$ resonances in transmission/reflection measurements," *Progress In Electromagnetics Research B*, Vol. 58, 95–109, 2014.
7. Hasar, U. C., "Self-calibrating transmission-reflection technique for constitutive parameters retrieval of materials," *IEEE Transactions on Microwave Theory and Techniques*, Vol. 66, 1081–1089, 2018.
8. Hasar, U. C., "Thickness-invariant complex permittivity retrieval from calibration-independent measurements," *IEEE Microwave and Wireless Components Letters*, Vol. 27, 201–203, 2017.
9. Baker-Jarvis, J., E. J. Vanzura, and W. A. Kissick, "Improved technique for determining complex permittivity with the transmission/reflection method," *IEEE Transactions on Microwave Theory and Techniques*, Vol. 38, 1096–1103, 1990.
10. Kato, Y., M. Horibe, M. Ameya, S. Kurokawa, and Y. Shimada, "New uncertainty analysis for permittivity measurements using the transmission/reflection method," *IEEE Transactions on Instrumentation and Measurement*, Vol. 64, 1748–1753, 2015.
11. Hasar, U. C., Y. Kaya, J. J. Barroso, and M. Ertugrul, "Determination of reference-plane invariant, thickness-independent, and broadband constitutive parameters of thin materials," *IEEE Transactions on Microwave Theory and Techniques*, Vol. 63, 2313–2321, 2015.
12. Kato, Y. and M. Horibe, "Improvement of transmission/reflection method for permittivity measurement using long fixtures with time-domain," *IEEE Transactions on Instrumentation and Measurement*, Vol. 66, 1201–1207, 2017.
13. Barry, W., "A broad-band, automated, stripline technique for the simultaneous measurement," *IEEE Transactions on Microwave Theory and Techniques*, Vol. 34, 80–84, 1986.
14. Baker-Jarvis, J., "Transmission/reflection and short-circuit line permittivity measurement," NIST Project, National Institute of Standards and Technology, Colorado, 1990.
15. Vector network analyzer uncertainty calculator, Keysight Software, version: 5.0.6.0, Jul. 2017.
16. Yamada, H., A. Meier, F. Mazzocchi, S. Schreck, and T. Scherer, "Dielectric properties of single crystalline diamond wafers with large area at microwave wavelengths," *Diamond and Related Materials*, Vol. 58, 1–4, 2015.
17. Thumm, M., "MPACVD-diamond windows for high-power and long-pulse millimeter wave transmission," *Diamond and Related Materials*, Vol. 10, 1692–1699, 2001.
18. Heidinger, R., G. Dammertz, A. Meier, and M. K. Thumm, "CVD diamond windows studied with low- and high-power millimeter waves," *IEEE Transactions on Plasma Science*, Vol. 30, 800–807, 2002.
19. Liu, Y. Q., M. H. Ding, J. J. Su, H. Ren, X. R. Lu, and W. Z. Tang, "An investigation on dielectric properties of diamond films in the range of K and Ka band," *Diamond and Related Materials*, Vol. 73, 114–120, 2017.
20. Hasar, U. C., "Self-calibrating transmission-reflection technique for constitutive parameters retrieval of materials," *IEEE Transactions on Microwave Theory and Techniques*, Vol. 66, 1081–1089, 2018.
21. Ding, M., Y. Liu, X. Lu, Y. Li, and W. Tang, "Boron doped diamond films: A microwave attenuation material with high thermal conductivity," *Applied Physics Letters*, Vol. 114, 162901, 2019.